Egyptian Journal of Phytopathology, Vol. 48. (2020) 71-80.
DOI: 10.21608/ejp.2020.49395.1015

ORIGINAL PAPER

Antifungal Activity of Silver Nanoparticles by *Trichoderma* species: Synthesis, Characterization and Biological Evaluation

El-Wakil, D. A.*[1&2]

Received: 10 November 2020 / **Accepted**: 10 December 2020 / **Published online**: 30 December 2020.

ABSTRACT

Synthesis of bio-nanoparticles is considered one of the most important trends for providing an eco-friendly method for nano compounds used in industry and biological purposes. Bio-nanoparticles are one of the safest important techniques. During the recent decades, many fungi have become serious and less likely to be treated with harmful fungicides, which are threatening human beings. The study tested *Trichoderma viride, T. hamatum, T. harzianum*, and *T. koningii* for the synthesis of biogenic silver nanoparticles. The bio-reduction of silver nanoparticles (AgNPs) was observed spectrophotometrically. The investigated AgNPs were characterized using ultraviolet-visible spectroscopy (UV-Vis) also, the transmission electron microscopy (TEM) and scanning electron microscopy (SEM) were followed. The synthesized AgNPs by *Trichoderma* spp. was observed and used as antifungal against four soil-borne *Fusarium* spp., *F. solani, F. semitectum, F. oxysporum* and *F. roseum*. The antifungal potency of AgNPs by *Trichoderma* species was evaluated against the investigated four *Fusarium* spp. which are considered serious soil-borne fungi.

Keywords: Bio-nanoparticles, *Trichoderma* spp., AgNPs, *Fusarium* spp., Antifungal activity.

***Correspondence: El-Wakil, D.A.**
E-mail: de107@yahoo.com

Deiaa A. El-Wakil
https://orcid.org/0000-0002-5854-8576

1- Plant Pathology Research Institute, Agricultural Research Center, 12619, Giza, Egypt.
2- Department of Biology, Faculty of Science, Jazan University, Kingdom of Saudi Arabia.

INTRODUCTION

Bio-nanoparticles are one of the safest important techniques around the world. During the recent decades, many fungi have become serious and less likely to be treated with harmful fungicides, which are threatens human beings. Fungicide-resistant microorganisms are emerging pathogens which resistance features pose a major challenge to containing their spread and their impact on different plants (Verma *et al*., 2010). Nanoparticles (NP) are usually a group of atoms in a size range from 1 to 100 nanometres (nm). It is understood that the properties of mineral NP are determined by their size, shape, composition, crystallization and structure. As an important mineral, silver nanoparticles (AgNPs) have a large number of applications (White *et al*., 2011). Nanoparticles have unparalleled physical, chemical, biological, and visual properties, and are used as antimicrobials in various fields. They also have many applications in optical devices, catalytic processes, biomarking, sensor technology and electronics (Schrand *et al*., 2008; Jain *et al.*, 2009; Govender *et al.*, 2010). Nanoparticles may suppress the expression of associated proteins with the production of adenosine triphosphate though some antimicrobial mechanisms affecting silver are not well understood (Liu *et al*., 1994 and Kabir *et al*., 2011). It was found that the exact dosages of silver and copper ions may kill bacteria in water, while higher doses of silver ions may be toxic to mammals (Kannan *et al.*, 2015). Different concentrations of silver nanoparticles synthesized by fungi were used by earlier workers in plant disease control (Vijayan *et al*., 2016). It has no harmful effects on humans e.g., as an alternative to synthetic fungicides, the use of AgNPs as antifungal agents have become more important and safer for environment. Application of AgNPs can be used to manage plant diseases (Ahmad *et al*., 2003 and Jain *et al.*, 2011). So far, there have been some reports of silver applications of nanoparticles against plant pathogens. Silver is increasingly used against plant diseases from the information about the antimicrobial activity of several silver compounds. Another requirement is to develop strategies to increase the application efficacy of AgNPs to suppress many plant pathogens (Huang *et al.*, 2007 and Jin, 2012).

The aim of the present study was to synthesize silver NPs and investigate their inhibitory effect against four *Fusarium* species infecting many plants leading to seedling damping-off and seed mortality (Ahmad *et al*., 2003).

MATERIALS AND METHODS

Source of fungal species:

During the present study, *Trichoderma viride, Trichoderma hamatum, Trichoderma harzianum* and *Trichoderma koningii* were isolated from Egyptian soil samples, identified (Dugan, 2017) by the Regional Centre for Mycology and Biotechnology Culture Collection Unit, at Al-Azhar University, Cairo Egypt, to investigate their AgNPs synthesizing capability as well as antifungal activity against four isolates of *Fusarium* spp., *i.e. F. solani, F. semitectum, F. oxysporum* and *F. roseum*, obtained from Plant Pathology Research Institute, Agricultural Research Center, Giza, Egypt.

Biomass preparation:

Each of *Trichoderma* species was grown on malt extract broth in flasks 100 mL at 25°C on a rotary shaker (120 rpm) for 96 hrs. Fungal biomass was briefly collected by filtration using Whatman filter paper No.1, followed by washing with distilled water to remove any unsuitable components of the medium. The biomass (2.5g) wet weight was placed in an individual flask containing 100 mL water and incubated at 25°C for 24 hrs. The biomass was filtered, and the cell filtrate was harvested and used for the process of biosynthesis of AgNPs (Bharde *et al*., 2006 and Devi and Joshi, 2012).

Biosynthesis of AgNPs, 50 mL of cell filtration were mixed with 10 mL of AgNO3 solution (1mM) and a reaction mixture without AgNO3 was used as a control. Preparations were incubated at 28°C for 24 hrs. Solutions were kept in the dark to avoid any photochemical reactions during the experiment. AgNPs were purified by centrifugation at 10,000 rpm for 10 minutes twice and collected for further characterization (Devi and Joshi, 2012).

Characterization of AgNPs:

Production of AgNPs in an aqueous solution was monitored at the Regional Centre for Mycology and Biotechnology using the following:

1- Analysis of UV-Visible Spectroscopy:

Change in colour of the filtrate incubated with silver nitrate solution was observed visually over some time. Absorption measurements of the filtrate were carried out after 24 hrs using a UV-visible between 200-300 nm (Milton-Roy Spectron 1201), Ingle *et al.* (2008).

2-Transmission Electron Microscopy (TEM):

Concerning TEM analysis, a drop of the cell filtrate was placed on the carbon-coated copper grids and dried by allowing water to evaporate at room temperature. Electron micrographs were obtained using JEOL JEM- 1010 transmission electron microscope (Japan) at 70 KV (Jain *et al.,* 2011).

3-Energy Dispersive Analysis of X-Ray (EDX):

The presence of elemental silver was confirmed through EDX. The EDX microanalysis was carried out by X-ray microanalyzer (Oxford 6587 INCA) attached to JEOL JSM-5500 LV scanning electron microscope (Jeol, Japan) at 20 KV. Sample filtrate was examined after drying on the specimen stubs and coated by gold coating on SPI-Module sputter coater and then examined under SEM on high mode under 15KV. The EDX spectrum was recorded in the spot profile mode from one of the densely populated silver nanoparticles region on the surface of the film (Devi *et al.,* 2012).

Fourier-Transform Infrared Spectroscopy (FTIR):

The FTIR spectra of biosynthesized AgNPs was recorded by KBr pellet method using JASCO FTIR-6200 with wavelength range 400-4000 cm^{-1} in transmission measuring mode.

X-Ray Diffraction (XRD):

The crystal phase information of the biosynthesized AgNPs was characterized from 10 to 80°C in 2θ by an X-ray diffractometer with CuK α radiation (Shimadzu XRD 6000, Japan), Sun and Xia, (2002).

Antifungal activity and minimum inhibitory concentration of AgNPs:

The agar well diffusion method was used. Sabouraud dextrose agar plates were seeded with the tested organisms; *Trichoderma viride, T. hamatum, T. harzianum* and *T. koningii*, and punched with a sterile Cork borer (0.6 cm diameter) to make open wells. AgNPs were added into the open wells at a concentration of 1mM. The plates were incubated at 28°C for 48 h. The experiment was carried out in triplicates and the average zone of inhibition in mm ± S.D was calculated. The lowest concentration of AgNPs which inhibited the growth of each tested microorganism was recorded using the broth dilution method (Wiegand *et al.,* 2008) as the minimum inhibitory concentration (MIC).

Morphological and ultrastructural studies:

Scanning electron microscopy of fungi treated with AgNPs

Fungal cells untreated (control) and treated with AgNPS at 0.25x MIC (detected from the

previous sections) were investigated morphologically using JEOL JSM-5500LV Scanning Electron Microscope (SEM) JEOL, Japan. Treated and untreated cells were prepared using an automatic tissue processor (Leica EM TP) where the samples were fixed in 2.5% glutaraldehyde and dehydrated using a series of ethanol washes (30, 50, 70, 90, and 100%). Samples were then dried using a critical point drier (Autosamdri-815) and then coated with gold using a gold sputter coater (SPI-Module) to be ready for mounting and examination **(**Suwalak and Voravuthikunchai, 2009).

Transmission electron microscopy of fungi treated with AgNPs:

Ultrastructure of *Trichoderma hamatum*, cells untreated (control) and treated with AgNPS at 0.25xMIC (detected from the previous section) was studied using JEOL JEM-1010 transmission electron microscope as the size of produced AgNPS of *Trichoderma hamatum* was the biggest relatively to other *Trichoderma* species. Samples were fixed in 1% osmium tetroxide in cacodylate buffer at room temperature for 1 hr. The cells were dehydrated in ethanol followed by acetone, then filtrated and embedded in Epon Epoxy resin. Then, samples were trimmed and cut into ultrathin sections using Leica Ultra cut UCT ultramicrotome. Ultrathin sections were stained with uranyl acetate and lead citrate, mounted on grids, then examined (Suwalak and Voravuthikunchai, 2009; Jain *et al*., 2011).

RESULTS AND DISCUSSION

Biosynthesis of silver nanoparticles (AgNPs)

The four fungal strains of *Trichoderma* spp. reduced silver salt into silver nanoparticles as noticed by visual observation of the fungal filtrate. The fungal filtrate exhibited a gradual change to a brown colour indicating formation of AgNPs. The colour of the culture filtrate with silver nitrate solution changed to intense brown after 24 hrs of incubation, while the control (without silver nitrate salt) did not exhibit any colour change as shown in Fig.1. These observations were noted also by Guilger *et al.* (2017), they reported that the synthesized nanoparticles showed bioactivity against many fungi which are attributed to new structures of different components especially when it used in biological evaluations.

Characterization of AgNPs

The UV-visible spectra of *Trichoderma viride, Trichoderma hamatum, Trichoderma harzianum* and *Trichoderma koningii* filtrate treated with silver nitrate showed characteristic surface plasmon absorption due to the formation of AgNPs at 424, 429, 433 and 435 nm, with *Trichoderma hamatum*, respectively (Fig.2). UV absorption spectra are essential way to monitor the formation and stability of metallic nanoparticles in aqueous solutions, such as the spectral response to nanoparticles depend on their diameter. The peak echo of the plasmon moves to longer wavelengths. It expands as the diameter increases. (Sun and Xia, 2002 and Shivaraj *et al.*, 2014). Therefore, the aqueous biosynthesis of silver ions can be successfully observed through UV-VIS rays, which are sensitive to many factors, such as particle shape, size, and interaction with the medium when synthesized the sample was subjected to UV spectroscopy (Shankar *et al.*, 2004 and Khan *et al*., 2013). The maximum value obtained was 400-500 nm, and the obtained results are in agreement with those obtained by Bansal *et al.*, 2011 and Elgorban *et al*. (2016).

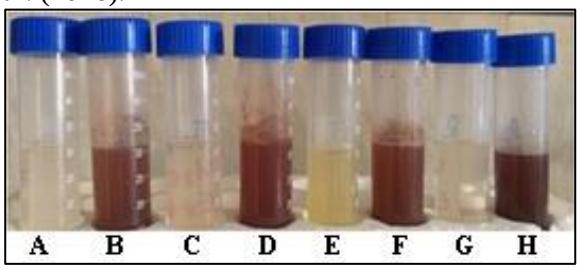

Figure (1): The Biosynthesis of silver nanoparticles, *Trichoderma viride* (A &B) control and with (AgNPs), *Trichoderma hamatum*, (C&D), control and with (AgNPs), *Trichoderma harzianum* (E&F) control and with (AgNPs) and *Trichoderma koningii* (G&H) control and with (AgNPs).

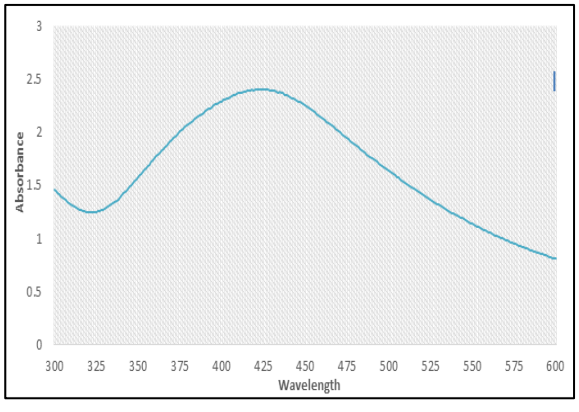

Figure (2): UV-visible absorption spectra for silver nanoparticles synthesized by *Trichoderma hamatum*. (RCMB 017005).

Transmission Electron Microscopy (TEM):

Electron micrograph was obtained using JEOL JEM-1010 transmission electron microscope as shown in Fig.3. Morphology and

size of complex silver nanoparticles were examined using TEM. The obtained photo (Fig.3) shows that compounded NPs have a spherical morphology, with a size range of 40 to 60 nm.

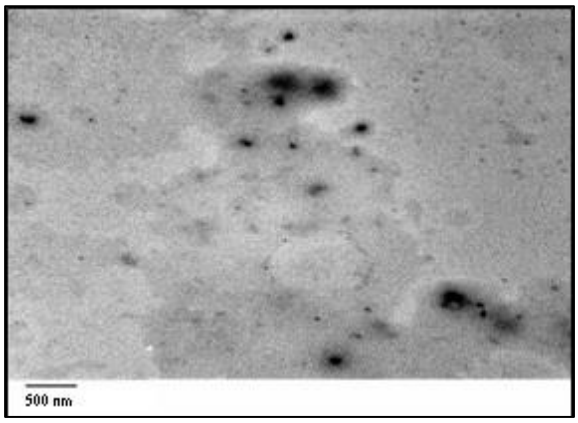

Figure (3): Transmission electron micrograph of synthesized silver nanoparticles. synthesized by *Trichoderma hamatum* of scale bar = 500nm.

Energy Dispersive Analysis of X-ray (EDX):

The EDX spectrum was recorded in the spot profile mode from one of the densely populated silver nanoparticles region on the surface of the film (Devi *et al.,* 2012). As shown in Fig.4. The EDX profile showed a strong Ag signal and weak carbon tops, which may be due to carbon tape used for analysis. The EDX spectrum revealed a clear identification of the component coil of the silver nanoparticles. The intense signal at 3 KeV strongly indicates that silver was the main component that showed optical absorption in this range, as a result of surface plasmon resonance. Such results are similar to those reported by other workers (Shankar *et al.,* 2004; Ingle *et al*., 2008; Mohanpuria *et al*., 2008 and Kim *et al*., 2009).

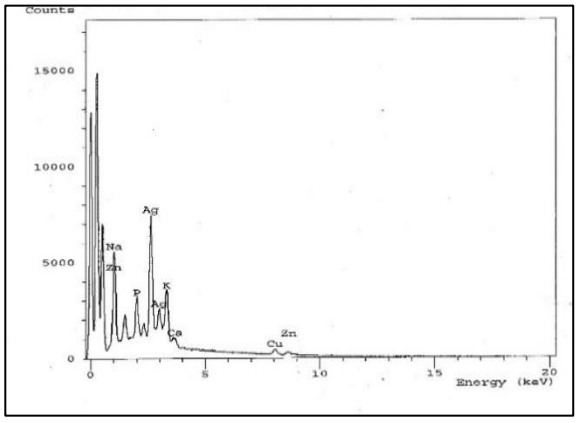

Figure (4): Showing EDX of AgNPs where scale bar =1 mm of *Trichoderma hamatum*

Fourier-transform infrared spectroscopy (FTIR):

The FTIR spectra of biosynthesized AgNPs were recorded by KBr pellet method using JASCO FTIR-6200 with wavelength range of 400 to 4000 cm^{-1} in transmission measuring mode as shown in Fig.5.The infrared spectroscopy cleared the peaks of elements of nanoparticles. Such observations agree with results recorded by many investigators (Huang *et al*., 2007; Ramanathan, *et al*., 2011 and Anna *et al*., 2015).

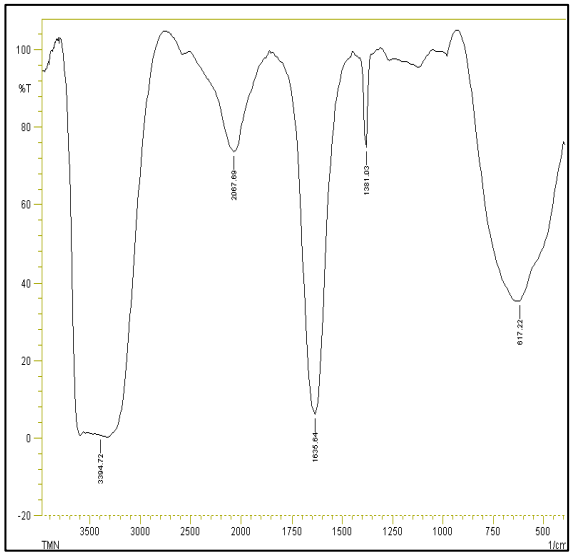

Figure (5): The IR of selected *Trichoderma hamatum* showing the peaks of infrared spectroscopy

X-Ray Diffraction (XRD):

The crystalline nature of the Ag NPs complex was confirmed by X-ray diffraction pattern analysis (XRD). Six clear reflections of the deviation were observed in 1.96480 ,2.65675, 3.20200, 3.68699, 4.10829 (Theta 10.000). The XRD pattern is shown in Fig 6. These results are cubic structure (fcc) cantered around the face is indicated by silver nanoparticles. These results are in agreement with those reported by Wiley *et al*. (2006); Mohanpuria *et al*. (2008); Schrand *et al*. (2008); Bansal *et al*. (2010); Bansal *et al*. (2011) and Elgorban *et al*. (2016).

Antifungal activity and minimum inhibitory concentration of AgNPs:

Antifungal activity and minimum inhibitory concentration of AgNPs were statistically measured by the size of AgNPs as measured by TEM (n=50). For *Trichoderma harzianum* (AgNPs) the mean size was 21.14, *Trichoderma viridi* (AgNPs) mean size was 18.63, *Trichoderma koningii* (AgNPs) mean size was 13.08. On the other hand, *Trichoderma hamatum* (AgNPs) recorded the highest measurement of the size at 72.86 (Table 1). All the tested fungal species showed a significant difference among isolates. Similar observations were recorded by Bharde *et al*., 2006; Narayanan and Sakthivel, 2010 and Devi and Joshi, 2012.

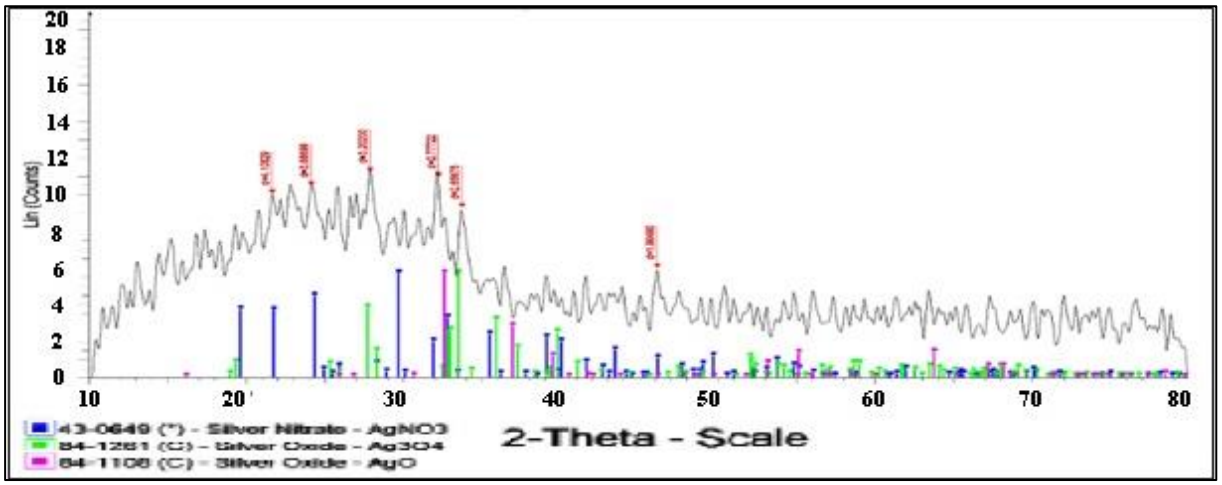

Figure (6): Scale values XRD of major synthesized bio-nanoparticles produced by selected *Trichoderma hamatum*.

Table (1): Statistical measurements of the size of AgNPs as measured by TEM (n=50).

Statistical Function	Diameter (nm)			
	T. harzianum AgNPs	*T. hamatum*, AgNPs	*T. viride* AgNPs	*T. koningii* AgNPs
Minimum size	11.78	49.53	9.43	9.94
Maximum size	33.64	91.52	38.78	20.76
Mean size	21.14	72.86	18.63	13.08
Standard Deviation	4.82	14.47	7.25	3.34
Count	50	50	50	50

The energy dispersive analysis of X-ray (EDX) of the elemental analysis of the four biosynthesized AgNPs:

Data in Table (2) show the Energy dispersive analysis X-Ray (EDX) of the elemental analysis of the four biosynthesized AgNPs. The highest percentage of Na was recorded with *Trichoderma hamatum* at 54.85 whereas P was observed with *Trichoderma koningii* at 14.93. Also, the element of K was observed at highest percentage with *T. koningii* (23.41%), Ca was recorded with *T. koningii* at 1.84%, and the highest percentage of Cu was recorded with *Trichoderma hamatum* at 3.84%, Zn was observed at 1.93 with *T. hamatum*, the highest percentage of Ag was recorded at 25.78 with *Trichoderma hamatum* also. These results are similar to those obtained by other researchers (Jain *et al*., 2009; Jin, 2012; Phanjom and Ahmed, 2017 and Siddiqi *et al.*, 2018), they discussed the biosynthesized AgNPs on different produced elements at different doses for creating a novel biosynthesized AgNPs material to employ it in different purposes in agriculture.

Table (2): Energy Dispersive Analysis of X-ray (EDX) showing the elemental analysis of the four biosynthesized AgNPs.

Element	Element %			
	T. harzianum AgNPs	*T. hamatum* AgNPs	*T. viride* AgNPs	*T. koningii* AgNPs
Na	53.91	54.85	52.96	47.36
P	11.84	9.17	10.23	14.93
K	21.38	14.68	19.04	23.41
Ca	0.74	1.29	1.47	1.84
Cu	2.17	3.84	1.89	0.13
Zn	0.00	1.93	0.00	0.00
Ag	8.63	25.78	14.25	4.87

Antifungal activities of biosynthesized AgNPs:

The antifungal activity of biosynthesized AgNPs against the investigated *Fusarium* species is shown in Table (3). The biosynthesized AgNPs of *Trichoderma hamatum* gave the highest inhibition zone by average 19.6mm against *Fusarium solani* relative to the control treatment, 10.6. The same trend was observed with *T. hamatum* against *F. semitectum* at (23.3mm) followed by *F. oxysporum* and *F. roseum* at the averages 19.3 & 21.6, respectively. On the other hand, *T. koningii* gave the least antifungal effect with the four investigated *Fusarium* species being 7.3, 8.6, 9.0 and 7.0 mm on the average, respectively compared with control for each fungus. Earlier workers investigated the antifungal activity of different biosynthesized AgNPs and stated that nano materials play an important role in suppressing each of the tested fungi if produced by microorganisms or medicinal plants (Vahabi *et al*., 2011; Devi *et al*., 2012; Pantidos and Horsfall, 2014; Alghuthaymi *et al.*, 2015; Vijayan *et al*., 2016; Guilger *et al*., 2017; Kamil *et.al.*, 2017; Liang *et al*., 2017 and Mohamed *et al*., 2017).

Table (3): Antifungal activities of biosynthesized AgNPs., the results are expressed as three readings of inhibition zone diameter in mm

Fungi	Inhibition Zone Diameter (mm)					
	T. harzianum AgNPs	*T. hamatum* AgNPs	*T. viride* AgNPs	*T. koningii* AgNPs	AgNO3 Control	Filtrate Control*
F. solani	8	22	7	8	11	-
	8	17	8	7	10	-
	7	20	7	7	11	-
Mean	7.6	19.6	7.3	7.3	10.6	0.0
F. semitectum	11	23	15	9	10	-
	10	21	16	8	12	-
	10	26	15	9	11	-
Mean	10.3	23.3	15.3	8.6	11	0.0
F. oxysporum	7	21	17	8	11	-
	7	18	15	9	9	-
	8	19	16	10	9	-
Mean	7.3	19.3	16.0	9.0	9.6	0.0
F. roseum	9	20	7	7	7	-
	10	24	7	7	8	-
	10	21	8	7	7	-
Mean	9.6	21.6	7.3	7.0	7.3	0.0

*The filtrate control that used for the biosynthesis of AgNPs for all the four fungi gave the same negative results.
AgNO3 control was tested at 1mM conc.
The samples were tested at 1mM conc.
The antifungal assay was performed using agar well diffusion assay.

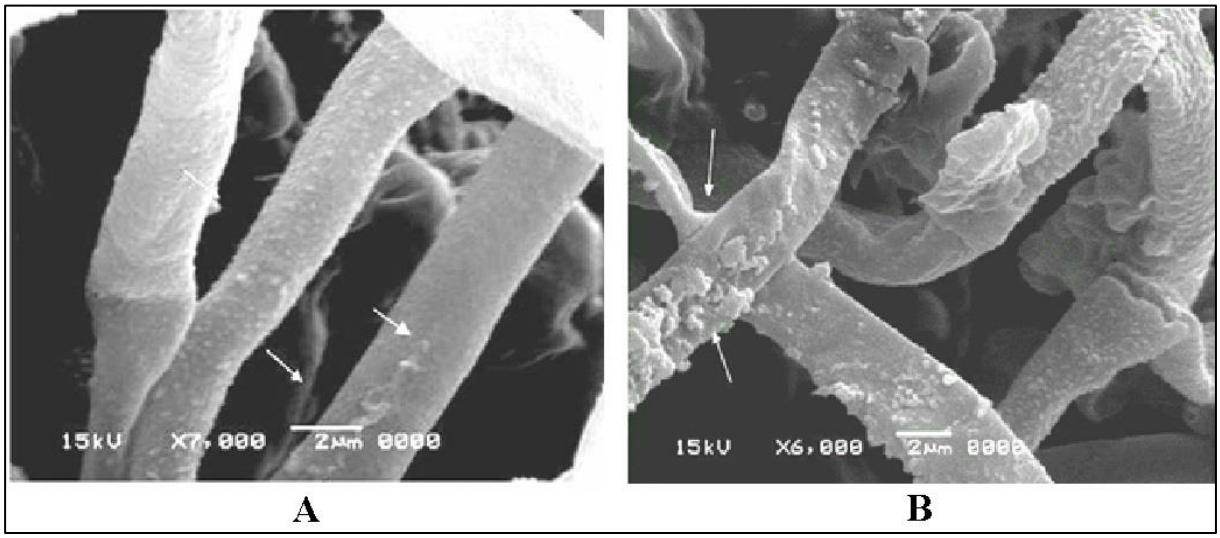

Figure (7): Scanning Electron Microscope photo showing the non-treated *T. hamatum* X 7,000 (A) and treated with AgNPs X 6, 000 (B) where the hyphae seem broken and deformed.

Scanning electron microscopy of fungi treated with AgNPs:

The plates obtained by SEM in Fig. (7) show a great variations between a non- treated *T.hamatum* X 7,000 (A) and treated with AgNPs X 6, 000 (B) scanned samples. Figure (A) shows the normal shape of fungal mycelium, whereas the treated sample with AgNPs at shape (B) shows aggregations of small micro nanoparticles at earlier stage of formation on the hyphae, Devi *et al*. (2012) and Mahdizadeh *et al*. (2015) obtained similar results.

Transmission electron microscopy of fungi treated with AgNPs:

Results obtained by TEM in Fig. (8) show a great variation between a non-treated sample of *T. hamatum* and treated ones in the plate (A). The granules and cell vacuoles, also the cytoplasmic components were detected, also dark grains of fungal structures were shown. On the other hand, in plate (B) treated one a transparent mycelium was shown due to treatment of AgNPs, the same observation was seen in plate (C) non-treated sample and in plate (D) treated mycelium. The study also showed that the fungal cell wall was affected by the treatment. These findings are in agreement with those reported by Jadhav *et al*., 2016. These results may propose that the use of biosynthesised AgNPs along with *Trichoderma* spp. could serve as effective green tools in order to inhibit the growth of pathogenic *Fusarium* spp. *in vitro* condition. Similar results were recorded by White *et al.* (2011) and Jadhav *et al*. (2016).

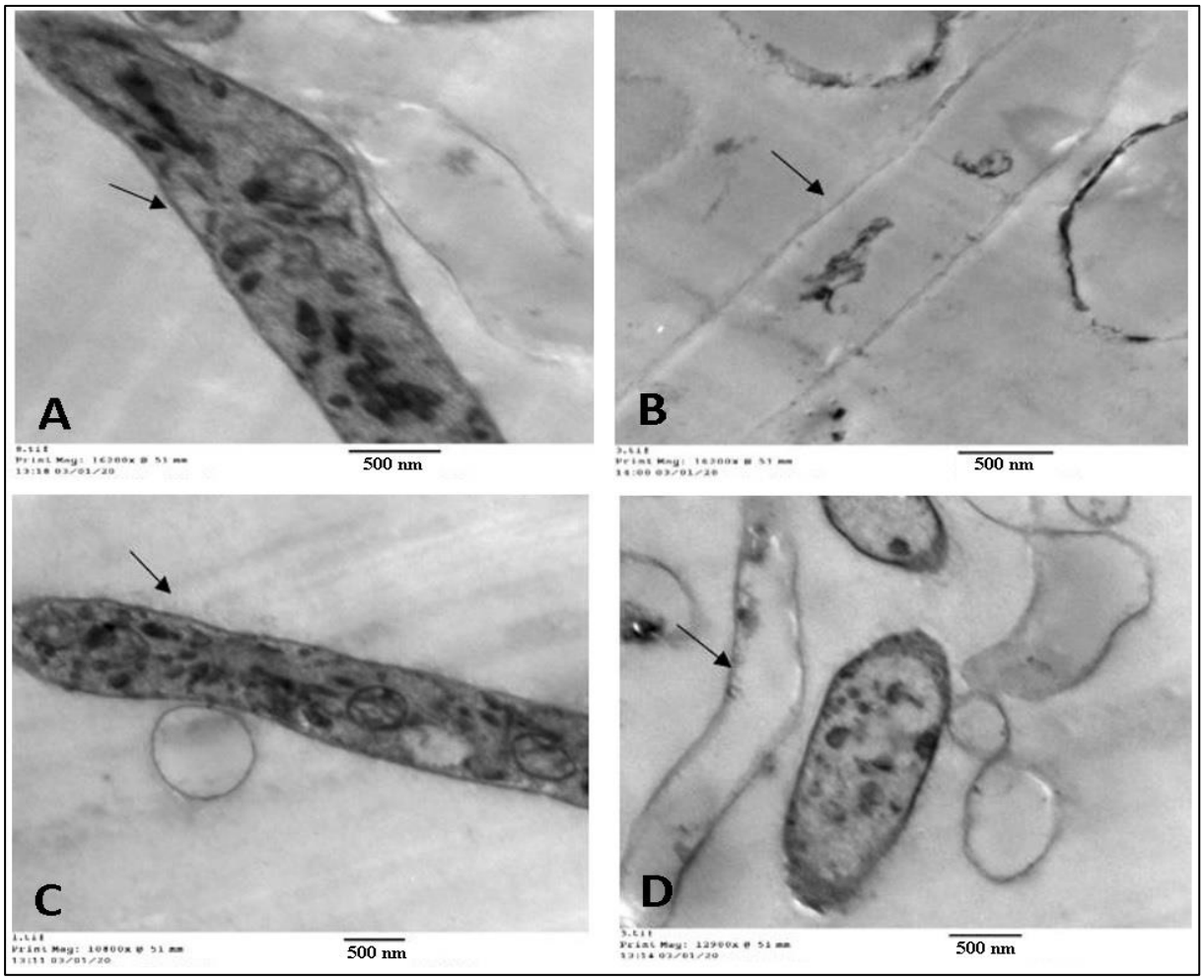

Figure (8): Transmission electron microscope photos show the non-treated *T. hamatum* (A &C) and treated with AgNPs (B & D). The vacuoles inside the hyphae and transparency of hyphae are noticed in plate B and plate D where the dark spots and granule accumulation are observed in plate A and plate C, untreated *T. hamatum.*

CONCLUSION:

The present study proved that nano biomaterials produced by *Trichoderma* species caused inhibitory effect against four plant pathogenic *Fusarium* species which are considered serious pathogens to many important field crops. The biosynthesized AgNPs of *Trichoderma hamatum* gave the highest effect against the four tested *Fusarium* spp.

ACKNOWLEDGMENTS:

The author would like to thank the researchers in the Regional Centre of Mycology and Biotechnology, Al-Azhar University, Cairo, Egypt for their advice and assistance during proceeding this work.

REFERENCES

Ahmad, A.; Mukherjee, P.; Senapati; S.; Mandal, D.; Khan, M.I; Kumar, R. and Sastry, M. 2003. Extracellular biosynthesis of silver nanoparticles using the fungus *Fusarium oxysporum*. Colloid Surface. Biochemistry and Molecular Biology, 28: 313-318.

Alghuthaymi, M.A; Almoammar, H.; Rai, M.; Said-Galiev, E. and Abd-El-Salam, K.A. 2015. Myco-nanoparticles: synthesis and their role in phytopathogens management. Biotechnology and Biotechnol. Equip., 29 (2): 221-236.

Anna, G.; Ewa, P. and Marek. K. and Marcin, N. 2015. Effect of nanosilver in wheat seedlings and *Fusarium culmorum* culture systems. Eur. J. Plant Pathol., 142 (2):251-261.

Bansal, V.; Ramanathan, R. and Bhargava, S.K. 2011. Fungus-mediated biological approaches towards "green" synthesis of oxide nanomaterials. Aust. J. Chem., 64(3): 279-293.

Bansal, V.L.; Vivian, L.; Mullane, A.P. and Bhargava, A.P. 2010. Shape dependent electrocatalytic behaviour of silver nanoparticles. Crystal. Eng. Comm., 12: 4280-4286.

Bharde, A.; Rautaray, D.; Bansal, V.; Ahmad, A.; Sarkar, I.; Yusuf, S.M. and Sanyal, M.S.M. and Sastry, M. 2006. Extracellular biosynthesis of magnetite using fungi. Indian Academy of Sciences 2, 135-141.

Devi, J.S.; Bhimba, B.V. and Ratnam, K. 2012. *In vitro* anticancer activity of silver nanoparticles synthesized using the extract of *Gelidiella* sp. Int. J. Pharm. Sci., 4(4): 710-715.

Devi, L.S. and Joshi, S.R. 2012. Antimicrobial and synergistic effects of silver nano-particles synthesized using soil fungi of high altitudes of eastern Himalaya. Microbiology, 40(1): 27-34.

Dugan, F.M. 2017. The Identification of Fungi: An Illustrated Introduction with Keys, Glossary, and Guide to Literature. The American Phytopathological Society (APS). 3340 Pilot Knob Road, St. Paul, MN 55121 USA.

Elgorban, A.M.; Abd El-Rahim, M.E.; Yassin, M.A.; Sayed, S.R.; Syed, F.A.; Elhindif, K.M.; Bakri, M. and Khan, M. 2016. Antifungal silver nanoparticles: synthesis, characterization and biological evaluation. Biotechnology & Biotechnological Equipment. 30(1): 56-62.

Govender, Y.; Riddin, T.L.; Gericke, M. and Whiteley, C.G. 2010. The enzymatic formation of platinum nanoparticles. J. Nanopart. Res.,12: 261-271.

Guilger, M.; Pasquto, T.; Bilesky-Joe, N.; Renato, P.C., Fernands. L. and Renata, D.L. 2017. Biogenic silver nanoparticles based on *Trichoderma harzianum*: synthesis, characterization, toxicity evaluation and biological activity. Scientific Reports. Vol. 7, Article No.44421.

Huang, J.L.; Li, Q.B.; Sun, D.H.; Lu, Y.H.; Su, Y.B.; Yang, X.; Wang, H.X.; Wang, Y.P.; Shao, W.Y.; He, N.; Hong, J. and Chen, C. 2007. Biosynthesis of silver and gold nanoparticles by novel sundried *Cinnamomum camphora* leaf. Nanotechnology. 18(10): 105-114.

Ingle, A.; Gade, A.; Pierrat, S.; Sonnichsen, C. and Rai, M. 2008. Mycosynthesis of silver nanoparticles using the fungus *Fusarium acuminatum* and its activity against some human pathogenic bacteria. Current Nanoscience, (4): 141-144.

Jadhav, K.; Dhamecha, D.; Bhattacharya, D. and Patil, M. 2016. Green and ecofriendly synthesis of silver nanoparticles: Characterization, biocompatibility studies and gel formulation for treatment of infections in burns. Journal of Photochemistry and Photobiology B: Biology, 155: 109-115.

Jain, J.A; Arora, S.; Rajwade, J.M.; Omary, P.; Kandelwal, S. and Panker, J.M. 2009. Silver nanoparticles in therapeutics: development of an antimicrobial gel formulation for topical use. Mol. Pharm., 6(5): 1388-1401.

Jain, N.; Bhargava, A.; Majumdar, S.; Tarafdar, J.C.; and Panwar, J. 2011. Extracellular biosynthesis and characterization of silver nanoparticles using *Aspergillus flavus* NJP08: a mechanism perspective. Nanoscale, 3(2): 635-641.

Jin, R. 2012. The impacts of nanotechnology on catalysis by precious metal nanoparticles. Nanotechnology Rev., 1: 31-56.

Kabir, L.; Sang, W.K.; Jin, H.J.; Yun, S.K.; Kyong, S.K. and Youn, S.L. 2011. Application of silver nanoparticles for the control of *Colletotrichum* species *in vitro* and

pepper anthracnose disease in field. Mycobiology, 39(3):194 -199.

Kamil, D.; Prameeladevi, T.; Ganesh, S.; Prabhakaran, N.; Nareshkumar, R and Thomas, S.P. 2017. Green synthesis of silver nanoparticles by entomopathogenic fungus *Beauveria bassiana* and their bioefficacy against mustard aphid (*Lipaphis erysimi* Kalt.). Indian Journal of Experimental Biology. 55: 555-561.

Kannan, B.; Narayanan, M.; Hyun, H.P. 2015. Antifungal activity of silver nanoparticles synthesized using turnip leaf extract (*Brassica rape* L.) against wood rotting pathogens. Eur. J. Plant Pathol. 140: 185-192.

Khan, M.; Khan, M.; Adil, S.F.; Tahir., M.N.; Alkhatlan, H.Z; Al-Warthan, A. and Siddique, M.R.H. 2013. Green synthesis of silver nanoparticles mediated by *Pulicaria glutinosa* extract. Int. J. Nanomedicine. 8:1507-1516.

Kim, S.W.; Kim, K.S.; Lamsal, K.; Kim, Y.J.; Kim, S.B.; Jung, M.; Sim, S.J.; Kim, H.S.; Chang, S.J.; Kim, J. K. and Lee, Y.S. 2009. An *in vitro* study of the antifungal effect of silver nanoparticles on oak wilt pathogen *Raffaelea* sp. Journal of Microbiology and Biotechnology, 19(8): 760-764.

Liang, M.; Wei, S.; Jian-Xin, L.; Xiao-Xi, Z.; Zhi, H.; Wen, L.; Zheng-Chun, L.; Jian-Xin, T. 2017. Optimization for extracellular biosynthesis of silver nanoparticles by *Penicillium aculeatum* and their antimicrobial activity and cytotoxic effect compared with silver ions. Mater. Sci. Eng., 77: 963-971.

Liu, Z.; Stout, J.E. and Tedesco, L. 1994. Controlled evaluation of copper-silver ionization in eradicating *Legionella pneumophila* from a hospital water distribution system. J. Infect. Dis., 169: 919.

Mahdizadeh, V.; Safaie, N. and Khelghatibana, F.A. 2015. Evaluation of antifungal activity of silver nanoparticles against some phytopathogenic fungi and *Trichoderma harzianum*. J. Crop Prot., 4(3): 291-300.

Mohamed, A.E.; Ismail, M.I.; Hisham, M.A. and Mohamed, Z. 2017. Identification and molecular characterization of Egyptian *Trichoderma* isolates. Bioscience Res., 14(4): 1156-1166.

Mohanpuria, P.; Rana, N.K. and Yadav, S.K. 2008. Biosynthesis of nanoparticles: Technological concepts and future applications. J. Nano Part. Res., 10: 507-517.

Narayanan, K.B. and Sakthivel, N. 2010. Biological synthesis of metal nanoparticles by microbes. Adv. Colloid Interface Science, 156; 1-13.

Pantidos, N. and Horsfall, L.E. 2014. Biological synthesis of metallic nanoparticles by bacteria, fungi and plants. J. Nanomedicine and Nanotechnology. 5: 1-10.

Phanjom, P. and Ahmed, G. 2017. Effect of different physicochemical conditions on the synthesis of silver nanoparticles using fungal cell filtrate of *Aspergillus oryzae* (MTCC No. 1846) and their antibacterial effects. Natural Sciences: Nanoscience Nanotech, 8: 1-13.

Ramanathan, R.; Mullane, P.O.; Parikh, R.Y; Smooker, P.M.; Bharava, S.K. and Bansal, V. 2011. Bacterial kinetics-controlled shape-directed biosynthesis of silver nanoplates using *Morganella psychrotolerans*. Langmuir. American Chemical Society, 27(2): 714-719.

Schrand, A.M.; Braydich-Stolle1, L.K.; John J.S.; Dai, L and Hussain, S.M. 2008. Can silver nanoparticles be useful as potential biological labels. Nanotechnol., 19(23): 5104.

Shankar, S.S.; Rai, A.; Ankamwar, B.; Singh, A.A. and Sastry, A.M. 2004. Biological synthesis of triangular gold Nanoprisms. Nat. Mater., 3: 482-488.

Shivaraj, N.A.; Vandana, R. and Dattu, S. 2014. Characterization and biosynthesis of silver nanoparticles using a fungus *Aspergillus niger*. International Letters of Nano Sciences, 15: 49-57.

Siddiqi, Q.S.; Husen, A. and Rao, R.A. 2018. Review on biosynthesis of silver nanoparticles and their biocidal properties. J. Nanobiotechnology, 16: 1-28.

Sun, Y.G. and Xia, Y.N. 2002. Shape-controlled synthesis of gold and silver nanoparticles. Science, 298: 2176-2179.

Suwalak, S. and Voravuthikunchai, S.P. 2009. Morphological and Ultrastructural changes in the cell structure of enterohaemorrhagic *Escherichia coli* following treatment with Quercus infected nut galls. Journal of Electron Microscopy, 58(5): 315-320.

Vahabi, K.; Mansoori, G.A. and Karimi, S. 2011. Biosynthesis of silver nanoparticles by fungus *Trichoderma reesei*. Sciences Journal. 1(1): 65-79.

Verma, V.C.; Kharwar, R.N. and Gange, A.C. 2010. Biosynthesis of antimicrobial silver nanoparticles by the endophytic fungus *Aspergillus clavatus.* Nanomedicine (Lond), 5: 33-40.

Vijayan, S.; Divya, K.; George, T.K. and Jisha, M.S. 2016. Biogenic synthesis of silver nanoparticles using endophytic fungi *Fusarium oxysporum* isolated from *Withania*

somnifera, its antibacterial and antitoxic activity. J. Bionanoscience, 10: 1-8.

Wiegand, I.; Hilpert, K. and Hancock, R.E. 2008. Agar and broth dilution methods to determine the minimal inhibitory concentration of antimicrobial substances. Nature Protocol, 3(2):163-175.

Wiley, B.J.; Im, S.H.; Li, Z.Y.; McLellan, J.; Siekkinen, A. and Xia, Y. 2006. Manoeuvring the surface plasmon resonance of silver nanostructures through shape-controlled synthesis. J. Phys. Chem., 110: 15666-15675.

White, R.J.; Budarin, V.L.; Moir, J.W. and Clark, J.H. 2011. A sweet killer: Mesoporous polysaccharide confined silver nanoparticles for antibacterial applications. Int. J. Mol. Sci., 12(2): 5782-5796.